Unique algorithm which takes into account source wave travel paths when estimating absorption values from DST data sets

Erick Baziw
Baziw Consulting Engineers Ltd., Vancouver, Canada
Gerald Verbeek
Baziw Consulting Engineers Ltd., Vancouver, Canada

ABSTRACT:
Dynamic soil analysis (DSA) in geotechnical practice is intimately related to the capability of measuring the necessary soil properties of shear modulus and absorption. In DSA the methods of analysis are based upon the stress-deformation response of soils due to imposed shear strains. Typically the soil profile is numerically modeled as linear visco-elastic system. This technique is referred to as the Equivalent Linear (EL) method, and it requires the specification of the input parameters of low-strain ($<10^{-5}$) shear modulus, modulus reduction, and the equivalent viscous damping ratio, which is directly related to the soil absorption value. Downhole seismic testing (DST) has proven to be a very accurate tool for estimating low strain shear modulus values as long as source wave raypaths are taken into account, especially for near-surface investigations. DST has also been utilized to estimate low-strain interval absorption values. In these cases standard frequency domain absorption estimation algorithms (such as the spectral ratio technique) are utilized where it is assumed that the source waves are traveling along the same travel path, which is obviously not the case for near surface DST investigations. This paper outlines a unique DST absorption estimation methodology, which is carried out in the time domain and takes into account source wave travel paths.

1. INTRODUCTION

There is considerable interest in methods of geotechnical *in-situ* engineering that provide accurate estimates of the shear wave velocity and the associated absorption values in the ground, since these parameters form the core of mathematical theorems to describe the elasticity/plasticity of soils and they are used to predict the soil response (settlement, liquefaction or failure) to imposed loads (whether from foundations, heavy equipment, earthquakes or explosions).

In dynamic soil analysis the methods are based upon the stress-deformation response of soils due to imposed shear strains (Finn, 1984; Idriss, 1990; Idriss and Sun, 1992; Ishihara, 1982; Kramer and Paulsen, 2004; Seed and Idriss, 1970; Wilson and Clough, 1962). A fundamental assumption made in the majority of these techniques is that soil deformations are a result of vertically propagating shear waves. Seed and Idriss (1970) implemented the wave equation with the assumption of harmonic vertically propagating shear waves. In this case a 2nd order linear visco-elastic system (also termed spring-mass-dashpot system) is assumed when numerically modeling soil response characteristics to dynamic loading. This technique is referred to as the Equivalent Linear (EL) method, which is the most commonly utilized ground modeling technique in practice (Kramer and Paulsen, 2004). The important parameters required within the EL method are the low-strain shear modulus (G_0), the modulus reduction and the equivalent

viscous shear damping ratio (η_s), which is proportional to the energy loss from a single cycle of shear deformation.

Downhole Seismic Testing (DST) has proven to be a very effective tool for the estimation of low the strain shear modulus G_0 (ASTM, 2017; Baziw, 2002; Baziw and Verbeek, 2012 and 2014). In a DST configuration a seismic source is used to generate a seismic wave train at the ground surface. One or more downhole seismic receivers are used to record the seismic wave train at predefined depth increments. These downhole receiver(s) may be positioned at selected test depths in a borehole or advanced as part of an instrumentation package as in the case of Seismic Cone Penetration Testing (SCPT). When triggered by the seismic source a data recording system records the response of the downhole receiver(s).

DST is also utilized for low strain estimation of the shear damping ratio η_s, which is important when predicting and assessing ground amplification during earthquakes (Stewart and Campanella, 1993). The low strain shear damping ratio is also used as a reference point for laboratory test results, such as Resonant Column Test data. This paper outlines a new technique for estimating η_s values from DST seismic data: the Forward Modeling Downhill Simplex Method Absorption Analysis (FMDSMAA). This technique utilizes several estimated in-situ parameters (such interval velocities, source wave travel paths, angles of incidence and reflection, density, and source wave amplitudes) when estimating absorption values, and takes the soil structure into account as up to eight absorption values (eight layers) are estimated simultaneously along with the geometric spreading exponent. The FMDSMAA technique provides automatically an error estimate, which is equal to the residual between the synthetic and measured amplitude ratios for each depth increment.

2. ABSORPTION ANALYSIS

Attenuation of a seismic wave propagating in soils is the decay of the wave amplitude in space (Aki and Richards, 2002; Gibowicz and Kijko, 1994; Sheriff and Geldart, 1982). Total attenuation arises from geometric spreading (due to the change in wave front), apparent attenuation (due to mode conversion, reflection-refraction at an interface) and material losses (intrinsic attenuation or absorption). In general terms, the earth acts as both a low pass filter and an attenuator as a seismic wave travels through it. The signal amplitude A within a homogeneous medium at distance x from the source is related to the amplitude A_0 at distance x_0 by

$$A(x) = A_0(x_0/x)^n e^{-\alpha(x-x_0)} \tag{1}$$

In (1) it is assumed that the decay is due to only geometric spreading and absorption. The *Quality Factor*, *Q*, is related to the absorption coefficient as follows:

$$Q = \pi/\alpha\lambda \tag{2}$$

In eq. (2) λ is the source wave's wavelength. The *Quality Factor* is a desirable term to define the absorption of a medium because it is nondispersive. The *logarithmic decrement,* δ, and *fraction of critical damping or damping ratio,* η, are expressed as

$$\delta = ln\left(\frac{amplitude}{amplitude\ one\ cycle\ later}\right) = \alpha\lambda = \pi/Q \tag{3}$$

$$\eta = \frac{\delta}{2\pi} = \frac{1}{2Q} \tag{4}$$

Tables 1 and 2 outline estimates of soil damping ratios for laboratory and field measurements, respectively

The amplitude decay term in eq. (1) $(x_0/x)^n$ corresponds to geometric spreading where $n = 1$ based upon the conservation of the energy flux of a traveling seismic wave and spherical divergence. Some researchers have noted that the amplitude of the seismic wave generally does not decay as $1/r$ where r is the travel distance and this why the exponent n is incorporated into eq. (1).

The apparent attenuation due refraction at an interface is quantified by the transmission coefficient, which quantifies the loss of energy when transitioning from layer 1 to layer 2 as outlined below in eq. (5).

$$T_{12} = \frac{A_2}{A_1} = \frac{2G_1\eta_1}{G_1\eta_1 + G_2\eta_2} = \frac{2Z_1}{Z_1 + Z_2} = \frac{\boldsymbol{2\rho_1 V_1 cos\theta_1}}{\boldsymbol{\rho_1 V_1 cos\theta_1 + \rho_2 V_2 cos\theta_2}} \tag{5}$$

In eq. (5) T_{12} is the transmission coefficient for the source traveling moving from layer 1 to 2, A_1 is the amplitude of incident wave, A_2 the amplitude of refracted wave, ρ_i is the medium density of layer i, θ_1 denotes the incident angle, θ_2 is the refraction angle, V_1 is the medium velocity of layer 1, V_2 is the medium velocity layer 2 (note: $Z_i = \rho_i V_i$ is the *acoustic impedance)*, G_i the shear modulus of medium i (note $G = \rho V_s^2$), and η_i is the vertical slowness within medium i. Note that the fractions of energy reflected ($E_R = R^2$ (where is the reflection coefficient)) and transmitted ($E_T = \frac{Z_2}{Z_1}T^2$) must add to one (i.e., $E_R + E_T = 1$).

.

Table 1: Laboratory measurements of soil damping (after Stewart and Campanella, 1993)

Soil Type	Strain (%)	Damping η_s (% Np)	Q (1/Np)	Q (1/dB)	Reference
Cohesive	10^{-3}	3(1-5)	16.7(50-10)	1.92(5.76-1.15)	*Sun et al. 1988*
Clay	10^{-3}	0.9-2.4	55.6-20.8	6.4-2.4	*Zavoral 1990*
Sand	10^{-3}	1.5	33.3	3.8	*Ishihara 1982*
Cohesionless	10^{-4}-10^{-3}	0.5-2	100-25	11.5-2.9	*Seed et al. 1986*
Sand	10^{-3}	1	50	5.8	*Saxena and Reddy 1989*

3.0 SPECTRAL RATIO TECHNIQUE

The Spectral Ratio Technique (SRT) is the most widely used method for determining Q or damping ratio from P or S waves acquired in the field (e.g., Rebollar, 1984; Campillo *et al.*, 1985; Redpath and Lee, 1986; Blakeslee *et al.*, 1989; Kvamme and Havskov,, 1989).

Table 2: Field measurements of soil damping (after Stewart and Campanella, 1993)

Soil Type	Damping η_s (% Np)	Reference
Sand	6	Kudo and Shima 1981
Silt	2.5	Kudo and Shima 1981
Alluvium (sand and clay)	12(<25m);3.5 (>25m)	B.B. Redpath (private communication) (laboratory: 1.5-3.5%)
Sandy	5	Tonouchi *et al.* 1983
Clayey	1.7	Tonouchi *et al.* 1983
Fine Sand	1.7	Tonouchi *et al.* 1983
Bay mud	2.5	Tonouchi *et al.* 1983
	4	B.B. Redpath (private communication) (laboratory: 2.5%)
Clay	4-7	Mok *et al.* 1988
Sand	2-3	Mok *et al.* 1988 (laboratory: 0.7%)

But the implementation of the SRT in DST has two major limitations: inaccurate raypath assumptions and spectral ratio estimation sensitivities. Although it is not necessarily emphasized, SRT assumes that the source waves travel along the same path.. While this may very well be the case for crosshole seismic testing (as shown in Fig. 1), it is certainly not the case for DST. Source wave trajectories adhere to *Fermat's principle*, which means that the raypath travels along the trajectory that minimizes the travel time between points, and that means that every depth the raypath will be different as shown in Fig.2 (Baziw 2002; Baziw and Verbeek 2012 and 2014).

Figure 1: Assumed source wave travel paths when implementing SRT.

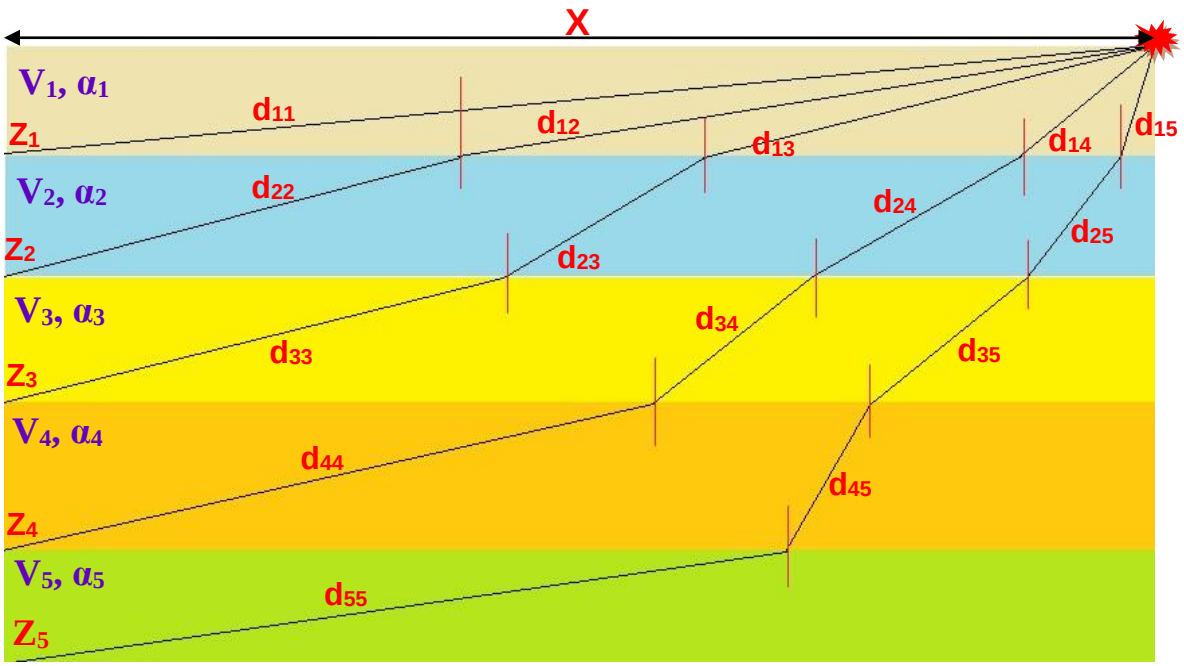

Figure 2: Near surface DST where SRT assumptions are not valid.

In addition SRT, just like any other frequency domain absorption estimation technique, can be highly susceptible to additive measurement noise or minor source wave distortions. This is best explained with an example. Figure 3 shows a wave (Wave 1) with a dominant frequency of 55 Hz that is assumed to be recorded at a vertical depth of 5m with a seismic source radial offset (X in Fig. 2) of 1.5m. Assuming that this wave travels through soil with a Q value of 30 Np^{-1} and a shear wave velocity of 153 m/s, the wave will reach a depth of 10 m 32 ms later (Wave 2). Figure 4 illustrates the output after applying the SRT on the traces illustrated in Fig. 3 and as is shown the derived Q value of 31.2 Np^{-1} is very close to the true value of 30 Np^{-1}. However, if a small amount of low frequency measurement noise is applied to Wave 1 and 2 (as illustrated in Fig. 5) the derived results change dramatically as shown in Fig 6: now the derived Q value of 6 Np^{-1} deviates significantly from the true Q value of 30 Np^{-1}.

Figures 7 and 8 illustrate a real data example of the challenges in applying the SRT. In this real data example SCPT seismic traces are acquired at depths of 3m and 15m as illustrated in Fig. 7. As is evident in Fig. 7, the maximum amplitude of the 3m traces is orders of magnitude greater than that of the 15m seismic trace. Figure 8 illustrates the results after applying the SRT on the traces illustrated in Fig. 7, generating a nonsensical estimate for Q of -66 Np^{-1}, implying that there was an increase in amplitude due to absorption as the source wave travelled to greater depths. In Fig. 7 rectangular time windows are applied to the full waveform seismic data under analysis so that spurious time series recordings and measurement noise are minimally incorporated into the spectral ratio analysis (Stewart & Campanella, 1993). The rectangular time window has an amplitude of 1.0 within a time span between t_1 and t_2. Start time t_1 is defined as the time location when moving back in time one zero crossing from the time index of the maximum pulse. End time t_2 is defined as the time location when moving forward in time two zero crossing from the time index of the maximum pulse.

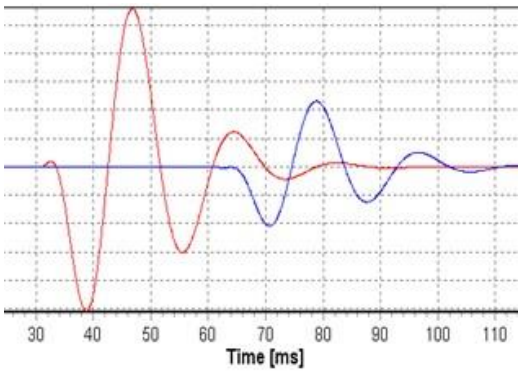

Figure 3. Source Wave 2 (in blue) superimposed on Source Wave 1 (in red) with 32 ms time offset.

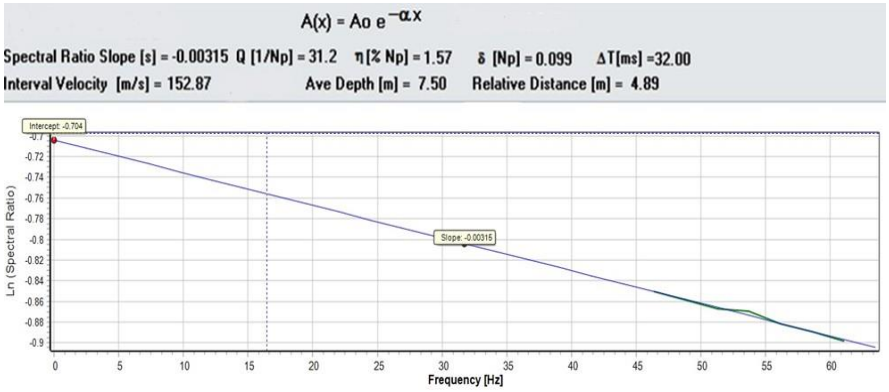

Figure 4: Output from SRT when processing the traces illustrated in Fig. 3. The estimated Q of 31.2 Np^{-1} is very close to the true Q value of 30 Np^{-1}.

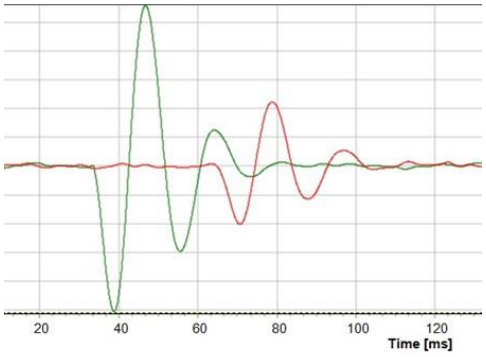

Figure 5. Traces illustrated in Fig. 3 with a small amount of additive measurement noise applied.

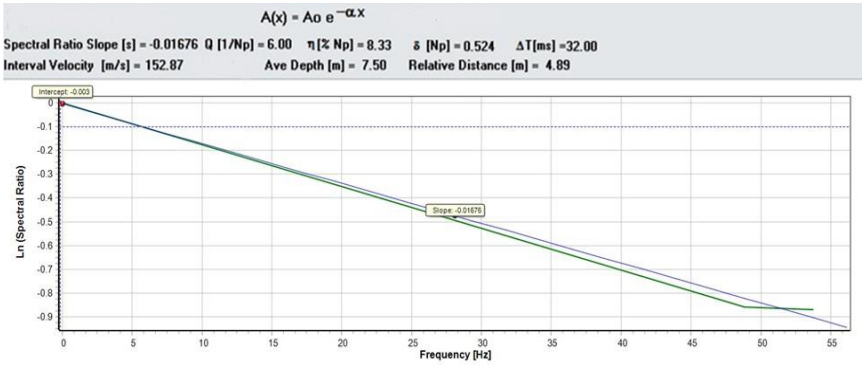

Figure 6. Output from SRT when processing the traces illustrated in Fig. 5. The estimated Q of 6 Np^{-1} deviates significantly from the true Q value of 30 Np.

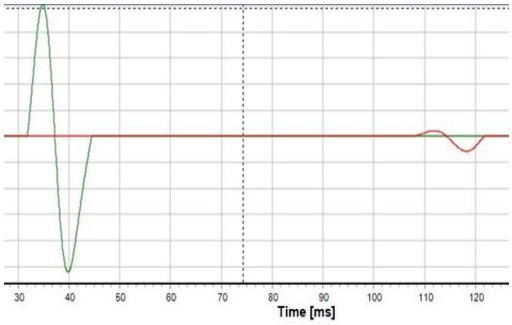

Figure 7. Real SCPT data with seismic traces acquired at 3m (green) and 15m (red).

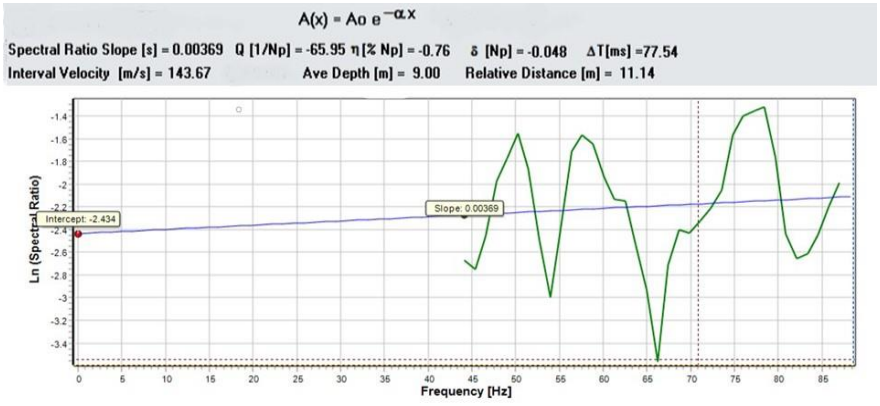

Figure 8. Output from SRT when processing the traces illustrated in Fig. 7. The SRT gives a nonsensical estimated Q of -66 Np^{-1}.

4.0 FMDSMAA TECHNIQUE

To address the SRT shortcomings a new algorithm was developed, which combines the Forward Modeling/Downhole Simplex Method (FMDSM) to ensure that the assumed raypaths are as accurate as possible with an Absorption Analysis (AA) that uses the absolute value of the full waveform amplitude as outlined in eq. (16).

$$|\rho(t)| = \sqrt{(X(t))^2 + (Y(t))^2 + (Z(t))^2} \tag{6}$$

where X(t), Y(t) and Z(t) are the orthogonal seismic sensor responses (where in case of an SH wave the Z(t) component can be ignored). The maximum $|\rho(t)|$ value is determined over the time window of the source wave responses, and it is obviously significantly simpler to obtain this full waveform maximum amplitude as opposed to rotating the X(t), Y(t) and Z(t) responses onto the full waveform, which is required for the SRT. Moreover, for low linearity traces source wave distortion can occur during rotation onto the full waveform, which can result in frequency distortion and poor SRT results as previously illustrated.

FMDMSAA technique utilizes several estimated in-situ parameters (such interval velocities, source wave travel paths, angles of incidence and reflection, density, and source wave amplitudes) when estimating absorption values, and it takes the soil structure into account as up to eight absorption values (eight layers) along with the geometric spreading exponent are estimated simultaneously. The FMDSMAA technique provides automatically an error estimate (i.e. the residual between the synthetic and measured amplitude ratios for each depth increment) and the algorithm allows for specification of minimum and maximum Q values to enhance the algorithm's performance.

4.1 FMDSMAA Algorithm Outline

The signal amplitudes for seismic traces recorded at various depths are defined utilizing eqs. (1) and (5) and the parameters illustrated in Fig. 2. In the subsequently outlined equations it assumed that there is an initial reference distance from the source of 0.1 m (i.e., $x_0 = 0.1m$ in eq. (1)). Equations (7), (8), (9), and (10) outlined below define the expected source amplitude for traces recorded at depths D_1, D_2, D_3, and D_4, respectively.

$$A_1 = A_0 \left(\frac{x_0}{d_{11}}\right)^n e^{-\alpha_1 (d_{11} - x_0)} \tag{7}$$

$$A_2 = T_{12} A_0 \left(\frac{x_0}{d_{12} + d_{22}}\right)^n e^{-(\alpha_1 (d_{12} - x_0) + \alpha_2 d_{22})} \tag{8}$$

$$A_3 = T_{23} T_{13} A_0 \left(\frac{x_0}{d_{13} + d_{23} + d_{33}}\right)^n e^{-(\alpha_1 (d_{13} - x_0) + \alpha_2 d_{23} + \alpha_3 d_{33})} \tag{9}$$

$$A_4 = T_{34} T_{24} T_{14} A_0 \left(\frac{x_0}{d_{14} + d_{24} + d_{34} + d_{44}}\right)^n e^{-(\alpha_1 (d_{14} - x_0) + \alpha_2 d_{24} + \alpha_3 d_{34} + \alpha_4 d_{44})} \tag{10}$$

In general terms, the amplitudes recorded at each subsequent DST depth of acquisition are mathematically expressed as follows:

$$A_i = A_0 \prod_{j=1}^{i-1} T_{ji} \left(x_0 / \sum_{j=1}^{i} d_{ji} \right)^n e^{-\left(\alpha_1 (d_{1i} - x_0) + \sum_{j=2}^{i} \alpha_j d_{ji}\right)}, \quad j \geq 1,\ i > 1 \tag{11}$$

If you then consider the ratio of the amplitudes, whether in absolute terms or globally normalized, the unknown amplitude A_0 drops out of the set of equations.

Based on the above the proposed FMDSM Absorption Algorithm (FMDSMAA) for estimating SH wave absorption coefficients can then be described as follows:

- Utilizing the standard interval velocity FMDSM technique (Baziw 2002; Baziw and Verbeek 2012 and 2014), obtain estimates of V_i, T_{ij}, and d_{ij}.

- For the depth increments under analysis determine the maximum amplitudes from the recorded amplitudes for each depth increment from the X and Y axes seismic recordings as follows:

$$A_i^m = max\left\{ \sum_{i=1}^{n} \sqrt{x^2(i) + y^2(i)} \right\} \tag{12}$$

- Specify the estimated densities for each depth interval based upon the CPTU recordings or known values. Typical density values are outlined below

Table 3: Approximate Material Properties (from ASTM D7128)

Material	*P*-Wave Velocity (m/s)	*S*-Wave Velocity (m/s)	Density (kg/m^3)
Dry sand/gravel	750	200	1800
Clay	900	300	2000
Saturated sand	1500	350	2100
Saturated clay	1800	400	2200
Shale	3500	1500	2500
Sandstone	2850	1400	2100
Limestone	4000	2200	2600
Granite	6000	3500	2600

- Implement FMDSMAA to calculate the synthesized amplitudes with eq. (11) based on assumed absorption coefficients, whereby the RMS difference between the measured and synthesizes amplitude ratios is minimized.

$$\min_{\alpha_i} \left\{ \sqrt{\sum_{i=1}^{n-1} \left(\frac{A_{i+1}}{A_i} - \frac{A_{i+1}^m}{A_i^m} \right)^2} \right\} \tag{13}$$

In eq. (13) n is the number of layers or absorption coefficients to be estimated.

It should be noted that when utilizing the FMSDMAA it is mandatory that the seismic source has the same energy output throughout the seismic profile

4.2 FMDSMAA - Test Bed Example:

Table 4 below provides the working parameters for a test bed simulation of the FMDSM-Absorption Algorithm (FMDSMAA). For a seismic wave with a frequency (*f*) of 100 Hz arrival times are assumed for 1-m thick soil layers down to a depth of 12 m. In addition for each soil layer values for the density and absorption coefficient are assumed.

Using FMDSM interval velocities (*V*) are then calculated for each depth interval, and with the outcome the wavelength is calculated ($V = f \times \lambda$). In addition the Quality factor is calculated ($Q = \pi/(\alpha \times \lambda)$). The source wave raypath diagram shown in Fig. 9 is used to calculate the incident and refraction angles, after which the globally normalized maximum amplitude is calculated using eq. (1) to account for absorption and geometric spreading as the source wave travels within a specific layer and the terms of eq. (5) (shown in bold font) to account for the energy loss as the source wave transitions from one layer to the subsequent deeper layer.

Table 4: FMDSMAA Test Bed Example Parameters (f = 100 Hz)

	Assumed			**Calculated**			
Depth **[m]**	**Arrival Time** **[ms]**	**Density** **ρ** **[kg/m^3]**	**Absorption** **α** **[1/m]**	**Interval Velocity** **v** **[m/s]**	**Wavelength** **λ** **[m]**	**Quality factor** **Q** **[1/** Np]	**Normalized Maximum Amplitude** **[m/s^2]**
1	17	1800	0.34129	131.5	1.32	7	1
2	25	1700	0.64708	97.1	0.97	5	0.45437
3	28	1600	0.162	176.3	1.76	11	0.341131
4	34	1400	0.275	142.8	1.43	8	0.235517
5	37	1500	0.05244	249.6	2.5	24	0.146707
6	41	1700	0.07431	222.5	2.23	19	0.111947
7	46	1600	0.1278	189.1	1.89	13	0.094043
8	49	1700	0.03701	303.2	3.05	28	0.061211
9	54	1800	0.10137	193.7	1.94	16	0.057829
10	58	1900	0.06177	242.2	2.42	21	0.042609
11	62	1500	0.05869	243.3	2.43	22	0.040829
12	65	1900	0.03048	322.1	3.23	32	0.027391

To validate the FMDSMAA the values shown in Table 4 for the arrival time, density, and the normalized maximum amplitudes are used as input data for the FMDSMAA. In addition the source wave raypath diagram shown in Fig. 9 was used to calculate the length and duration for each segment of the various raypaths. With these values the absorption was derived for each depth, after which the Quality Factor and the Damping Factor were determined as well. Table 5 outlines the output of the FMDSMAA where the calculated and assumed values for the absorption, the Quality Factor and the Damping Factor show very close agreement with the initial test bed values, which demonstrates the FMDSMAA's correctness.

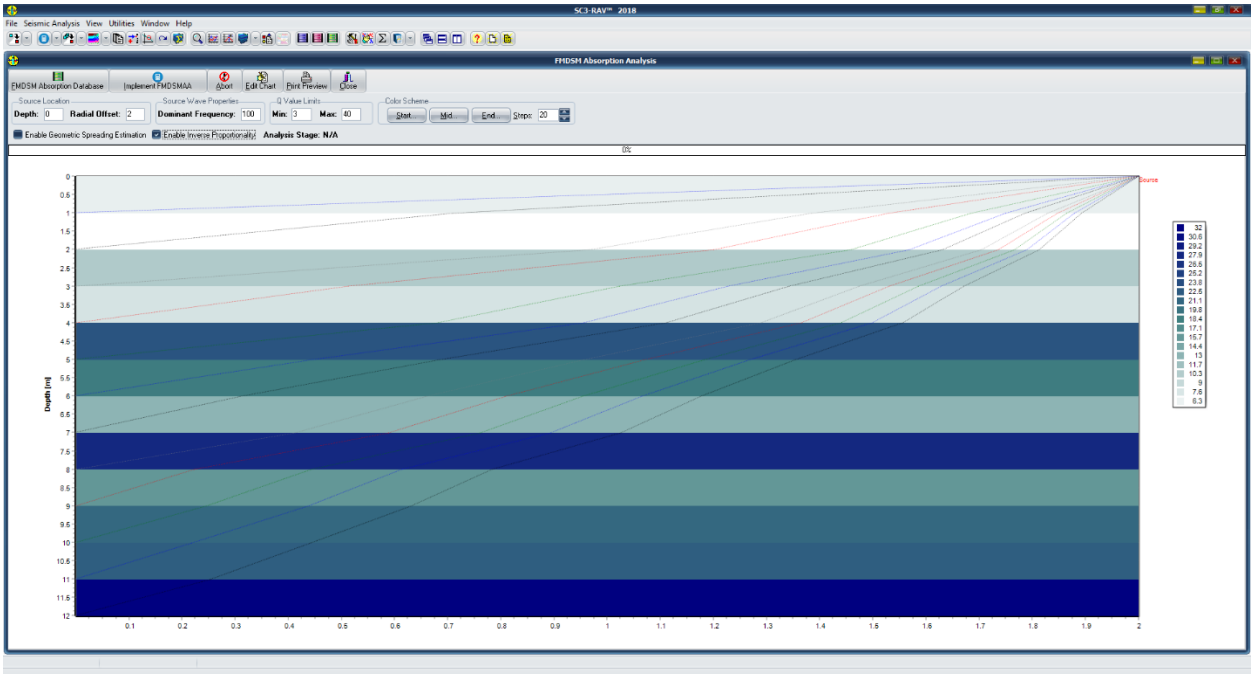

Figure 9: DST illustrating twelve simulated source waves as input into the FMDSMAA test bed analysis.

Table 5. FMDSMAA Test Bed Example Results

Depth **[m]**	**Assumed Absorption** **α** **[1/m]**	**Calculated Absorption** **α*** **[1/m]**	**Q Based on α** **[1/** Np]	**Q* Based on α*** **[1/** Np]	**η* Damping Based on Q*** **[% Np]**
1	0.34129	0.36115	7	6.6	7.59
2	0.64708	0.65681	5	4.9	10.14
3	0.162	0.16951	11	10.5	4.75
4	0.275	0.27762	8	7.9	6.32
5	0.05244	0.05449	24	23.1	2.17
6	0.07431	0.07514	19	18.8	2.66
7	0.1278	0.12823	13	13	3.86
8	0.03701	0.0374	28	27.7	1.8
9	0.10137	0.10154	16	16	3.13
10	0.06177	0.06191	21	21	2.38
11	0.05869	0.05879	22	22	2.27
12	0.03048	0.03054	32	32	1.56

CONCLUSIONS

This paper has outlined a unique DST absorption estimation methodology, which is carried out in the time domain and takes into account source wave travel paths. This new technique is referred to as the Forward Modeling Downhill Simplex Method Absorption Analysis (FMDSMAA), and it utilizes several estimated in-situ parameters (such interval velocities, source wave travel paths, angles of incidence and reflection, density, and source wave

amplitudes) when estimating absorption values. The FMDSMAA technique automatically provides for an error estimate, which is equal to the residual between the synthetic and measured source wave amplitudes for each depth increment. The implementation and performance of the FMDSMAA algorithm was demonstrated by considering a challenging test bed example. In a future paper the authors intend to demonstrate the algorithm with actual field data and compare it with the spectral ratio technique, which should further demonstrate the validity of this new technique.

REFERENCES

Aki, K. and Richards, P.G. (2002), Quantitative Seismology, 2nd edition, Sausalito, California: University Science Books.

ASTM (American Standards and Testing Methods). (2017). "D7400: Standard Test Methods for Downhole Seismic Testing." ASTM Vol. 4.09 Soil and Rock (II): D5877-latest.

ASTM (American Standards and Testing Methods). (2017). "D7128: Standard Guide for Using the Seismic-Reflection Method for Shallow Subsurface Investigation." ASTM Vol. 4.09 Soil and Rock (II): D5877-latest.

Baziw, E., and Verbeek, G. (2012). "Deriving Interval Velocities from Downhole Seismic Data", Geotechnical and Geophysical Site Characterization 4 – Mayne (eds), CRC Press, 1019–1024.

Baziw, E. (2002), "Derivation of Seismic Cone Interval Velocities Utilizing Forward Modeling and the Downhill Simplex Method", Can. Geotech. J., 39(5), pp.1181-1192.

Baziw, E. and Verbeek, G. (2014). "Identifying Critical Layers using SCPT and Seismic Source Moveout." In the Proceedings of the 3rd International Symposium on Cone Penetration Testing, CPT'14, May 12-14, 2014 - Las Vegas, Nevada, 357-364.

Blakeslee, S., Malin, P., and Alvarez, M. (1989), "Fault-zone attenuation of high-frequency seismic waves", Geophys. Res. Lett. 16, 1321-1324.

Capillo, M., Plantet, J.L., and Bouchon, M, (1985), "Frequency-dependent attenuation in the crust beneath central France Lg waves: Data analysis and numerical modeling", Bull. Seism. Soc. Am. 75, 1395-1411.

Finn, W.D.L. (1984). Dynamic response analysis of soils in engineering practice. In Mechanics of engineering materials. John Wiley & Sons Ltd., New York. Chapter 13.

Gibowicz, S.J. and Kijko, A. (1994), An Introduction to Mining Seismology, Academic Press Inc.

Idriss, I.M. (1990), "Response of soft soil sites during earthquakes," Proc. H. Bolton Seed Memorial Symposium, J.M. Duncan (ed.), Vol. 2, 273–290.

Idriss, I.M. and J.I. Sun (1992). SHAKE91: A computer program for conducting equivalent linear seismic response analyses of horizontally layered soil deposits, Center for Geotech. Modeling, Univ. of Calif., Davis.

Ishihara, K. (1982), "Evaluation of soil properties for use in earthquake response analysis", International Symposium on Numerical Models in Geomechanics, Zurich, pp. 237-259.

Kramer, S.L. and S.B. Paulsen (2004), "Practical use of geotechnical site response models", Proc. Int. Workshop on Uncertainties in Nonlinear Soil Properties and their Impact on Modeling Dynamic Soil Response, PEER Center Headquarters, Richmond, CA.

Kudo, K., and Shima, E. (1981), "Attenuation of shear waves in soil. In Seismic wave attenuation", edited by M.N. Toksoz and D.H. Johnston. Geophysics Reprint Series No. 2. Society of Exploration Geophysics, Tulsa, Okla., 325-338.

Kvamme, L.B., and Havskov, J. (1989), "Q in Southern Norway", Bull. Seism. Soc. Am. 79, 1575-1588.

Redpath, B.B., and Lee, R.C., 1986, In-situ Measurements of Shear Wave Attenuation at a Strong Motion Recording Site: Report Prepared for USGS Contract No. 14-08-001-21823.

Mok, Y.J., Sanchez-Salinero, I., Stokoe, K.H., and Roesset, J.M. (1988),."In situ damping measurements by crosshole seismic method", In Earthquake Engineering and Soil Dynamics 11. Proceedings, ASCE Specialty Conference, Park City, Utah. Geotechnical Special Publication No. 20, 305-320.

Rebollar, C. J. (1984), "Calculation of Qβ using spectral ratio method in Northern Baja California", Bull. Seism. Soc. Am. 74 , 1371-1382.

Saxena, S.K., and Reddy, K.R. (1989), "Dynamic moduli and damping ratios for Monterey No. 0 sand by resonant column method", Soils and Foundations, 29(2): 37-51.

Seed, H. B. & Idriss, I. M. (1970), "Soil moduli and damping factors for dynamic response analyses", Earthquake Engineering Research Center, College of Engineering, University of California - Berkeley California, Report No. EERC 70-10.

Seed, H.B., Wong, R.T., Idriss, I.M., and Tokimatsu, K. (1986), ”Moduli and damping factors for dynamic analyses of cohesionless soils”, ASCE Journal of the Geotechnical Engineering Division, 112: 1016-1032.
Sheriff, R.E. and Geldart, L.P. (1982), Exploration Seismology, Vol. 1, (2nd ed.) Cambridge, UK: Cambridge University Press.
Stewart, W.P., and Campanella, R.G. (1993), “Practical aspects of in-situ measurements of material damping with the seismic cone penetration test”, Can. Geotech. J. 30, 211 219.
Sun, J.I., Golesorkhi, R., and Seed, H.B. (1988), "Dynamic moduli and damping ratios for cohesive soils", Report UCB/EERC-88/ 15, University of California, Berkeley.
Toksoz, M.N., Johnston, D.H. and Timur, A. (1979), "Attenuation of seismic waves in dry and saturated rocks: I. Laboratory measurements", Geophysics Vol. 44, 681-690.
Tonouchi, K., Sakayama, T., and Imai, T. (1983), “ S wave velocity in the ground and the damping factor”, Bull. IAEG. No.26-27, pp.327-333. WOODS, R.D. and STOKOE, K.H.II. 1985. Shallow seismic exploration in soil dynamics. Richart Commemorative Lectures, ASCE. 120-156
White, J.E. (1965) Seismic waves. McGraw-Hill, New York.
Wilson, E.L. & Clough, R.W. (1962), “Dynamic response by step-by-step matrix analysis”, Symposium on the Use of Computers in Civil Engineering, Laboratorie Nacional de Engenharia Civil, Lisbon - Portugal, pp. 45.1 - 45.14.
Zavoral, D. (1990), Dynamic properties of an undisturbed clay from resonant column tests, M.A.Sc. thesis, Department of Civil Engineering, University of British Columbia, Vancouver.